Optics & Laser Technology 165 (2023) 109618

Contents lists available at ScienceDirect

Optics and Laser Technology

journal homepage: www.elsevier.com/locate/optlastec

Full length article

Timing jitter reduction of CW-LD-pumped 1.34 μm high-repetition-rate Nd:YVO_4/V:YAG laser with optimal spatial overlap rate

Yanxin Shen [a,b], Xihong Fu [a,*], Xinpeng Fu [a], Cong Yao [a,b], Wenyuan Li [a,b], Jun Zhang [a], Yongqiang Ning [a]

[a] State Key Laboratory of Luminescence and Applications, Changchun Institute of Optics, Fine Mechanics and Physics, Chinese Academy of Sciences, Changchun 130033, China

[b] University of Chinese Academy of Sciences, Beijing 100049, China

ARTICLE INFO

Keywords:
High-repetition-rate
1.34 μm
Passively Q-switched
Spatial overlap effect
Simulation

ABSTRACT

In this work, we investigated the characteristics of a continuous-wave (CW) laser diode (LD) end-pumped 1.34 μm passively Q-switched Nd:YVO_4/V:YAG laser experimentally and theoretically. A four-level theoretical model for 1.34 μm passively Q-switched Nd:YVO_4/V:YAG laser which includes the non-radiative transition, the effective pump power, the spatial overlap effect and the thermal lens effect was demonstrated to give a transcendental equation that can accurately reflect the output characteristics of the laser. Based on the theoretical analysis, the spatial overlap rate was further optimized, we finally realized high-repetition-rate pulse output with time jitter of 180 ns at 220 kHz repetition rate and 200 ns at 357 kHz repetition rate. The good agreement between the experiment results and theoretical model provides a reference for the accurate prediction of the output characteristics of 1342 nm passively Q-switched laser.

1. Introduction

1.3 μm laser has been used in various fields, such as communication、detection、biosensing, and so on [1–3]. According to the ANSI Z136.1-2014 standard, the allowable power of the 1.34 μm laser is 1.9 times that of the 1.5 μm and 18 times that of the 910 nm laser in the range of Class 1 power. So, it has important potential application value in the field of laser radar [4]. Passively Q-switching is one of the effective ways to obtain pulsed laser. Compared with actively Q-switched, it has a simpler structure, lower cost, and smaller size. Because $NdYVO_4$ crystal has a large stimulated emission cross-section at 1.34 μm (7.6×10^{-19} cm^{-2}) and absorption coefficient (31.4 cm^{-1}) [5,6]. LD pumped $NdYVO_4$ crystal is a common way to obtain a 1.3 μm laser. Researchers have done a lot of works on 1.3 μm passively Q-switched Nd:YVO_4 lasers [7]. In 2005 Lai et al. used InAs/GaAs quantum dot material as a saturable absorber (SA), an average output power of 360 mW with a Q-switched pulse width of 90 ns at a pulse repetition rate of 770 kHz was obtained. [8]. In 2017 Lin et al. reported a 214 kHz passively Q-switched $NdYVO_4$ based on graphene-oxide SA, the pulse duration was 322 ns, and the corresponding peak power was 7.39 W[9]. In 2020 Kane et al. demonstrated a 1.82 MHz 1.3 μm laser with 4.8 ns pulse duration and 68 W peak power [4]. Under pulsed pumping conditions, a time jitter of 1 % at 11 kHz output was achieved, while for higher repetition rates the time jitter was ± 20 %. It showed the promise of the stable output of a high-repetition-rate 1.3 μm passively Q-switched laser.

The research suggests that the strong pulse-to-pulse amplitude and repetition rate jitters frequently observed in the diode pumped solid-state lasers could be an intrinsic nature of the system[10]. Researchers have proposed a lot of technical means to improve the stability of passively Q-switched laser output, the three main techniques are as follows:: 1. pulse LD pumping, the pulse period and pulse width are much smaller than the upper level lifetime, the number of upper level inversion population in the gain medium increases step by step, which can keep the laser in a relatively stable state[4,11–13]. 2. The gain pre-pumping technology, the direct-current component keeps the number of inversion particles in the gain medium close to threshold until the Q switch is turned on. The pulse component causes the number of inversion particles to increase rapidly and the Q-switch to turn on quickly [14,15]. However, the two technologies require strict control of pulse interval, pulse waveform, increasing system complexity and usage cost. 3. In the external optical modulation, another LD is used to irradiate the

* Corresponding author.
E-mail addresses: shenyanxin20@163.com (Y. Shen), fuxh@ciomp.ac.cn (X. Fu), fuxp@ciomp.ac.cn (X. Fu).

https://doi.org/10.1016/j.optlastec.2023.109618
Received 22 February 2023; Received in revised form 25 April 2023; Accepted 16 May 2023
Available online 27 May 2023

SA, the SA can be quickly drifted in a short time, the Q switch is quickly switched on [16,17], this requires an additional LD and control circuit, which cannot achieve a compact structure and increases the cost. In addition, there are self-seeding input method、ring cavity, multi-mirror and other technologies[18–20]. These technologies require additional devices, structures and extreme requirements for circuits. In summary, these techniques are mainly classified into two types: stabilizing the Q-switch and suppressing the mode competition. However, there are few studies on the influence of mode matching on the time jitter of high repetition rate pulses. It has been found that mode matching can improve output properties such as beam quality and light-to-light conversion efficiency. Therefore, we believe that pulse stability can also be improved by optimizing mode matching without adding other devices.

In this work, we compress the time jitter of 1.34 μm passively Q-switched laser by mode matching. Firstly, a $NdYVO_4$ laser was presented to produce high-repetition-rate pulse output. When the pump power raised from 2.18 W to 4.5 W, the repetition frequency was increased from 130 kHz to 357 kHz. Secondly, we studied the influence of the spatial overlap effect on the stability of 1.34 μm pulses output and the resonant cavity was optimized according to the theoretical predictions. In this way, we achieved 180 ns time jitter at 220 kHz and 200 ns time jitter at 357 kHz. Finally, the passively Q-switched rate equation was further extended to describe and guide the experiment more accurately, the effects of SA, output coupler (OC) mirror, pump power and the spatial overlap effect on laser output characteristics were studied by numerical simulation. The theory was consistent with the experiment. At present, there are few studies on the time jitter of 1.34 μm passively Q-switched laser. This work was of good reference to the analysis and experiment of 1.34 μm passively Q-switched laser.

2. Experiment setup

The experiment setup of 1.34 μm passively Q-switched laser is showed in Fig. 1(a). A 6 W 808 nm fiber-coupler LD with a core diameter of 105 μm and numerical aperture of 0.22 was employed as the pump source, which was focused into Nd:YVO_4 crystal by a couple of lenses with a compression ratio of 1:1. The gain medium was 1 at.% Nd:YVO_4 crystal with a dimension of $3 \times 3 \times 3$ m^3. It was wrapped with indium foil and fixed in a TEC-cooled copper heat sink. The input side of $NdYVO_4$ crystal was high transmittance coated at 808 nm and high reflection coated at 1.34 μm. A V:YAG $3 \times 3 \times 0.5$ m^3 was employed as a saturable absorber with small-signal transmission $T_0 = 90$ %. The reflectivity of the output coupler mirror was 91 % at 1.34 μm. The cavity length was 15 mm. The power was measured by a thermal laser power meter (S425C-L, THORLABS Inc., USA). A digital oscilloscope (DS1104, RIGOL Inc., CHINA) and InGaAs photodetector (DET08CFC, THORLABS Inc., USA) were used to record the temporal shape of the output laser pulse and the repetition rate. The laser spectrum was measured by an optical spectrum analyzer (AQ6370D, YOKOGAMA Inc., JPN) as presented in Fig. 1(b).

3. Spatial overlap effect

The spatial overlap between the pumping and lasing was changed by the variation of the F2 position, as shown in Fig. 2(a). d3 is the distance between the F2 and the input side of the Nd:YVO_4. Z_0 is the distance between the incident face of the crystal and the pump beam waist. ω_{p0} is the radius at the pump beam waist. Z_0 and ω_{p0} changed with d3 from 8.25 mm to 10.5 mm. Fig. 2 (b) shows the relationship between the time jitter and Z_0 of 1.34 μm passively Q-switched laser at a repetition rate above 200 kHz. Since the refractive index of a crystal is different from that of air, the waist position moves at different intervals inside and outside the crystal. It can be seen from the Fig. 2(b) that the pulse time jitter is small when the beam waist is in the range of 0.5 to 1.5 mm, and the experimental results of the position marked by red circle in Fig. 2(b) are shown in Fig. 2(c). The pulse time jitter was 180 ns and the average pulse width was 7.7 ns when the beam waist was located at 0.75 mm. When the waist of the pump beam was outside the crystal, the maximum time jitter was 700 ns and the average pulse width was 8.4 ns.

The spatial overlap rate between pump and laser modes affects the efficiency of the output power M^2 factor and the stability of the laser oscillator[21,22]. When the laser is operated at low power, mode matching requires that the size of the pump light should be smaller than or equal to the size of the oscillating light. In high-power runs, large fundamental mode radius can significantly increase the thermally induced diffraction losses due to higher-order spherical aberration due to thermal effects. The size of the pump light should be larger than the size of the oscillating light. The effective mode volume V_{eff} and spatial overlap coefficient η_0 are defined as [23]:

$$V_{eff} = \left(\iiint s_l(x,y,z) r_p(x,y,z) dv \right)^{-1} \tag{6}$$

$$\eta_0 = \frac{\left(\iiint s_l(x,y,z) r_p(x,y,z) dv \right)^2}{\left(\iiint s_l^2(x,y,z) r_p(x,y,z) dv \right)} \tag{7}$$

Where $s_l(x,y,z)$ and $r_p(x,y,z)$ are the normalized cavity mode intensity distribution and the normalized cavity mode intensity distribution, respectively. From Fig. 3, it is obvious to observe the effect of Z_0 and ω_{p0} on the spatial overlap, when Z_0 is in the range of 0.5–1 mm, the spatial overlap rate of pump light and oscillating light is high. This conclusion is in agreement with experimental results, which demonstrate that it is easier to achieve relatively stable operation of the laser when the overlap between the Gaussian beam of the pump and the fundamental mode light in the cavity is high. At a pump power of 3.2 W, the optimal location of pump beam waist of 0.5 mm can be obtained by numerical simulation with the highest spatial overlap coefficient of 38.2 %. In the experiment, the time jitter at the same position was 200 ns.

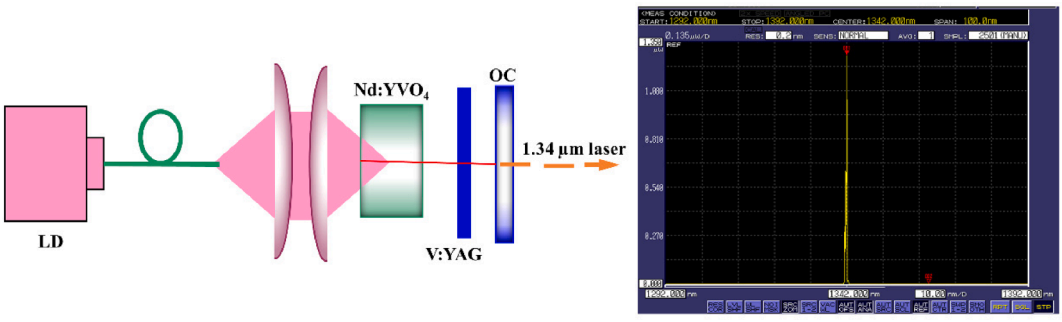

(a) (b)

Fig. 1. (a) The schematic of 1.34 μm laser. LD: laser diode, OC: output coupler mirror; (b) 1342 nm laser spectrum measurement.

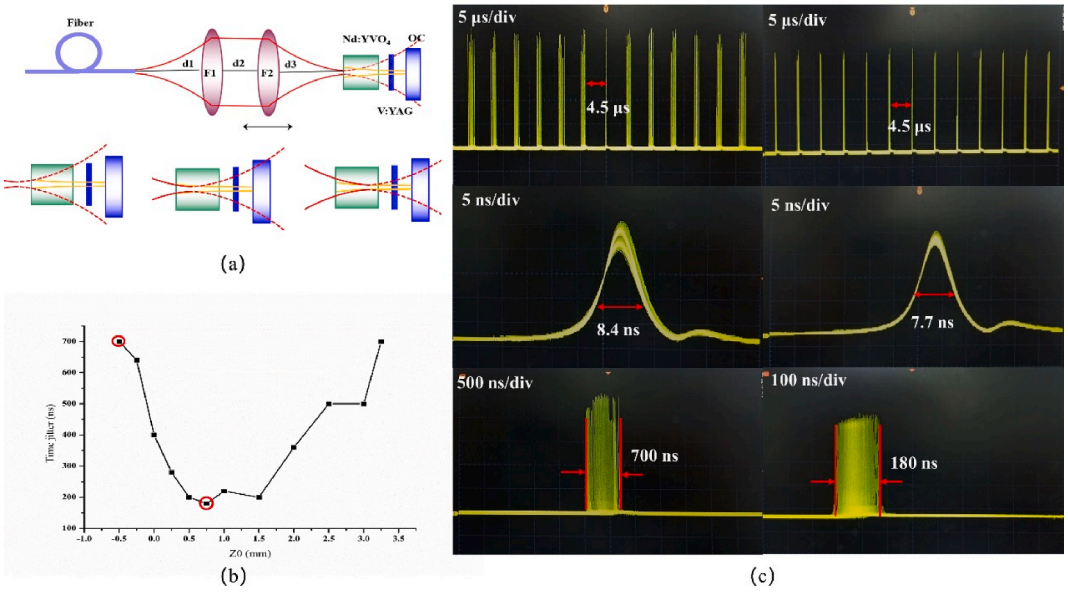

Fig. 2. Experiment results (a) Schematic diagram of two coaxially arranged gaussian mode matching, F1、F2: focus lens (f = 10 mm), OC: output coupler mirror, d1、d2、d3: the distance between adjacent devices. (b) the time jitter at different positions; (c) the envelope oscilloscope traces pulses, multi-pulse oscilloscope traces, pulse time jitter range.

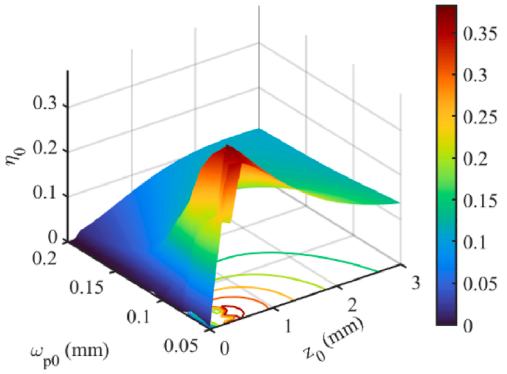

Fig. 3. Variation of spatial overlap coefficient η_0 with pump beam waist radiusω_{p0} and its position Z_0 in the gain medium.

4. Theory analysis and experimental results

To describe the passively Q-switched laser more accurately, we used the four-level model based on the laser rate equations [10,24]. The number of active ions in the gain medium and the non-radiative transitions between energy levels are also considered. Not all of the pump energy is absorbed by the crystal, and some of the absorbed pump energy is turned into heat due to quantum defects. In view of these factors, the laser rate equation can be extended as follows:

$$\frac{d\varphi}{dt}=\frac{\varphi}{t_r}\left[2\sigma_g l_g(N_2-N_1)-2\sigma_{gs}l_s N_{gs}-2\sigma_{es}l_s\left(N_{s0}-N_{gs}\right)-\ln\left(\frac{1}{R}+L\right)\right] \tag{1}$$

$$\frac{dN_2}{dt}=P_{in}\left(\frac{1-\exp(-\sigma_{abs}N_0 l)}{h\nu\pi\overline{\omega}_{p0}^2 l}\right)-(\gamma_{20}+\gamma_{21})N_2-\gamma\sigma c\varphi(N_2-N_1) \tag{2}$$

$$\frac{dN_1}{dt}=-\gamma_{10}N_1+\gamma_{21}N_2+\gamma\sigma c\varphi(N_2-N_1) \tag{3}$$

$$\frac{dN_0}{dt}=\gamma_{20}N_2+\gamma_{10}N_1-P_{in}\left(\frac{1-exp(-\sigma_{abs}N_0 l)}{h\nu\pi\overline{\omega}_p^2 l}\right) \tag{4}$$

$$\frac{dN_{gs}}{dt}=\gamma_s\left(N_{s0}-N_{gs}\right)-\frac{A_g}{A_s}\sigma_{gs}c\varphi N_{gs} \tag{5}$$

Where φ is the intracavity photonic densities, $N_{(0,1,2)}$ are the instantaneous population densities in upper, lower and ground laser transition states. According to [25], the total active ion ($N_1+N_2+N_0=1.25\times10^{26}/m^3$) in the gain medium are calculated. σ_g and σ_{abs} are the stimulated emission cross-section and stimulated absorption cross-sections of the gain medium, respectively. σ_{gs} and σ_{es} are absorber ground and excited state absorption cross-sections, respectively. $\gamma=1$ is the inversion reduction factor of four-level, $\gamma_{20}\gamma_{10}\gamma_{21}$ are the decay rates of the energy levels. γ_s is the saturable absorption recovery rate. L is the round-trip dissipative loss. l_s is the SA length,l is the length of the resonator cavity, l_g is the gain medium length, c is the velocity of light, $t_r=2l'/c$ is the round-trip time of light in the resonator cavity of optical length where $l'=n_g l_g+n_s l_s+l-l_g-l_s$. n_g is the refractive of crystal, n_s is the refractive of SA, $N_{s0}=-\ln(T_0)/(\sigma_{gs}\bullet l_s)$ is the total population densities of SA, N_{gs} and N_{es} are the ground and excited state population densities, respectively. The relation between them is $N_{s0}=N_{gs}+N_{es}$. T_0 is the small signal transmission of the SA. R is the reflectivity of the OC. The analysis of the crystal thermal lensing effect is also essential given the influence of the crystal thermal effect on the laser performance. For the theoretical thermal modeling of CW end-pumped solid-state laser, the thermal focal lens is given by the approximate expression[26] $f_T=\frac{2\pi\overline{\omega_{p0}}^2K}{P\xi\beta}\bullet\frac{1}{dn/dT+\alpha_T n_g}$, where K is the thermal conductivity, dn/dT is the thermal-optical coefficient, α_T is the thermal expansion coefficient, P is the pump power, ξ is the thermal load ratio, $\beta=1-\exp(-\sigma_{abs}N_0 l_g)$ is the absorption rate of pump light by the crystal[27],$\overline{\omega_{p0}}$ is the average radius of pump mode in the gain medium. So, the effective pump power is expressed as $P_{in}=P\bullet(1-\xi)$, $h\nu$ is the photonic energy, the pump rate is given by $P_{in}\left(\frac{1-exp(-\sigma_{abs}N_0 l_g)}{h\nu\pi\overline{\omega_{p0}}^2 l}\right)$. A_g/A_s is the effective area ratio of gain medium to SA. ω_g is the average radius of cavity mode in the gain medium,ω_s is the average radius of cavity mode in the SA. The mode size with a distance z away from the beam waist can be expressed as $\omega(z)=\omega_0\sqrt{1+\left(\frac{z\lambda}{\pi n_{g,s}\omega_0^2}\right)^2}$, the beam waist ω_0 was calculated by the ABCD matrix. According to the related parameters in Table 1, the numerical

Table 1
The parameters of the numerical simulation.

Parameters	Values	Parameters	Values
σ_g	7.6×10^{-19} cm^{-2}[5]	ξ	0.24[26]
σ_{abs}	2.5×10^{-19} cm^{-2} [27]	K	5.2 $W{\cdot}m^{-1}{\cdot}K^{-1}$[26]
σ_{gs}	7.2×10^{-18} cm^{-2} [5]	dn/dT	3×10^{-6} K^{-1}[26]
σ_{es}	7.4×10^{-19} cm^{-2} [5]	α_T	4.43×10^{-6} K^{-1}[26]
γ	1	n_g	2.2[26]
γ_s	4.55×10^{7} s^{-1}[5]	n_s	1.82[5]
γ_{20}	3359.74 s^{-1}[10]	c	3×10^{8} $m{\cdot}s^{-1}$
γ_{21}	4731.33 s^{-1}[10]	h	6.626×10^{-34} J·s
γ_{10}	5×10^{7} s^{-1}[10]	λ	1342 nm
l_g	3 mm	λ_p	808 nm
l_s	0.5 mm	L	0.04
l	15 mm		

simulation was carried out..

According to [24,28–30], the single-pulse energy E and the peak power Pmax can be described as follows:

$$E = \frac{h\nu A\eta_0}{2\sigma\gamma}\ln\left(\frac{1}{R}\right)\ln\frac{N_i}{N_f} \tag{8}$$

$$P_{max} = \frac{h\nu A l^{'}}{t_r}\ln\left(\frac{1}{R}\right)\varphi_{max} \tag{9}$$

Where A is the effective area of cavity mode, η_0 is the spatial overlap coefficient, N_i and N_f are the initial and final inversion population density of the gain medium. The average output power P_{mean} is calculated by $P_{mean} = E \bullet f_{rep}$, f_{rep} is the pulse repetition rate.

Fig. 4 shows the numerical simulation results, they present the relationship between laser output characteristics and SA initial transmittance T_0, OC mirror reflectivity R. When the pump power P = 3.2 W, the average radius of pump mode $\overline{\omega_{p0}}$ = 92μm, the pulse repetition rate and pulse width increase with the increase of T_0 and R, but it is obviously to found that peak power dramatically decrease with the raising of T_0 and R. It could be easy to know that higher transmittance of OC mirror and SA leads to a larger average output power. In this work, T_0 = 90% SA and R = 91% OC mirror were used to achieve high repetition rate pulse output.

The three-dimensional surface diagram in Fig. 5 is the numerical simulation results, showing the relationship between the laser output characteristics and the pump power P, the average radius of pump mode $\overline{\omega_{p0}}$. The red scattered dots in Fig. 5 show the experiment results. As the pump power was changed from 2.18 W to 4.5 W, the average output power and the repetition rate increased from 250 mW to 410 mW, and from 130 kHz to 357 kHz,respectively. The peak power decreased from 229 W to 125 W as the pump power increases. But the variation of pulse width was small (about 7–8.5 ns). Because the variation of $\overline{\omega_{p0}}$ can affect the size of ω_g and ω_s, overlap efficiency and the second threshold condition will also be changed, the laser output properties will change dramatically. In this experiment, when a passively Q-switched laser was operated in the chaotic regime, the jitter of the pulse will cause the laser output properties to deviate from the ideal value, with output power smaller and pulse width larger than the ideal state. It demonstrates that pulse jitter can cause severe deterioration of the laser output properties.

Based on the above simulation and experimental results, by further optimizing and tuning the resonator, a laser with a repetition rate of 357 kHz, time jitter of 200 ns, the average pulse duration of 7.2 ns, output power of 410 mW was realized at 4.5 W pump power, as shown in Fig. 6.

5. Conclusion

Pulse jitter is an intrinsic property of LD pumped passively Q-switched lasers, which is more serious in high-repetition-rate pulse output. When the passively Q-switched laser operates at a high repetition rate, the gain and loss in the cavity change rapidly, resulting in fluctuations of the Q-switched state. Improving the coupling efficiency reduces the energy loss and the generation of other modes, thus enhancing the stability of the cavity. In this work, the effect of spatial

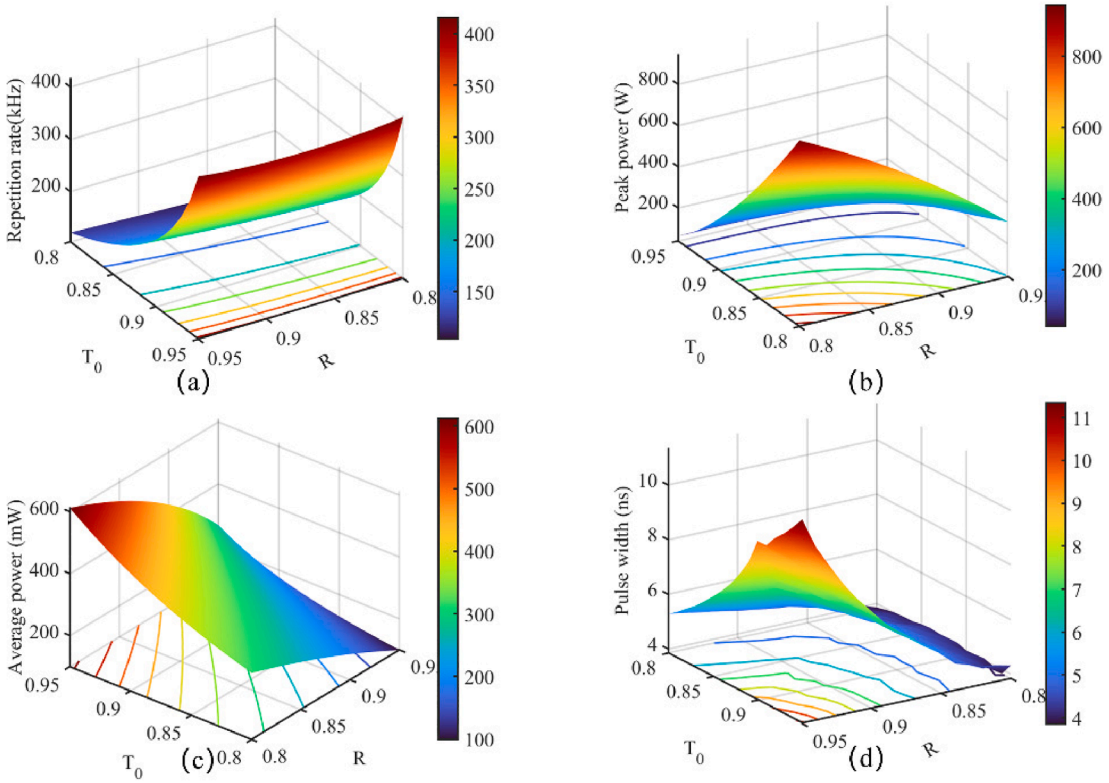

Fig. 4. Repetition rate(a), the peak power(b), the average output power (c), the pulse width(d) versus SA initial transmittance T_0 and OC mirror reflectivity R.

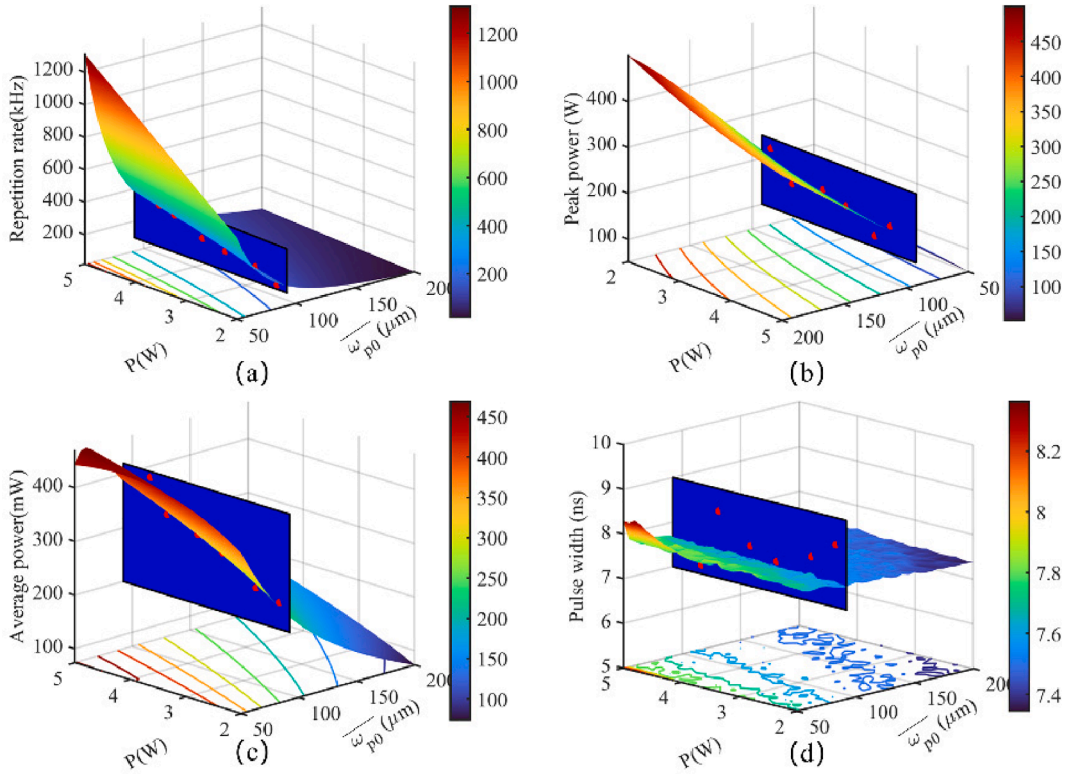

Fig. 5. Repetition rate(a), the peak power(b), the average output power (c), the pulse width(d) versus pump power P and the average radius of pump mode $\overline{\omega_{p0}}$; red scattered dots, experiment results; surface diagram, numerical simulation results. (For interpretation of the references to colour in this figure legend, the reader is referred to the web version of this article.)

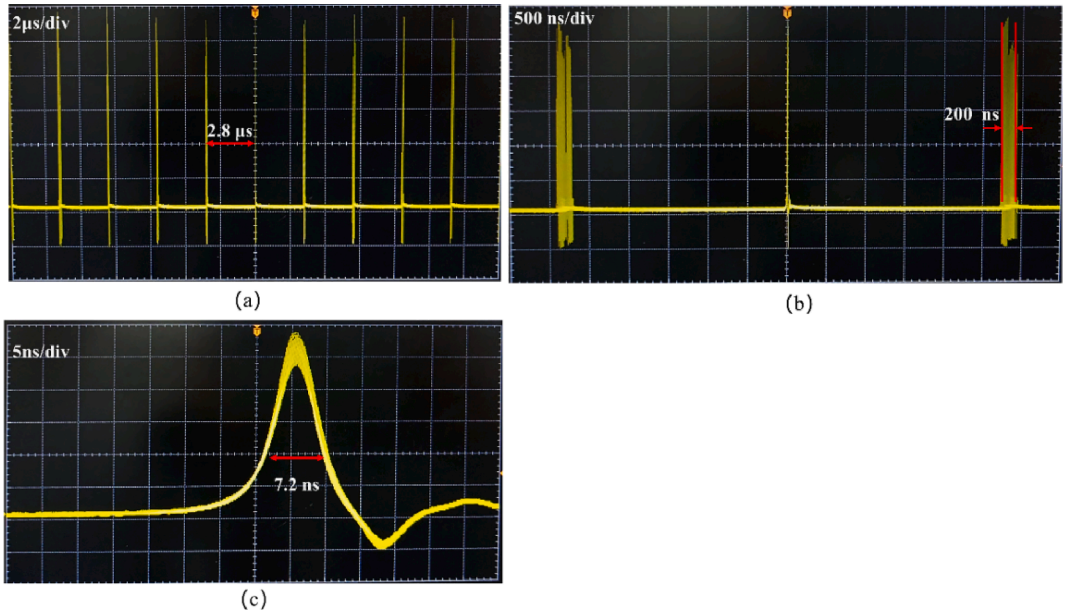

Fig. 6. Experiment results (a) the envelope oscilloscope traces pulses; (b) pulse time jitter range; (c) multi-pulse oscilloscope traces.

overlap on laser performance is studied both theoretically and experimentally. The laser rate equations are extended to model passively Q-switched laser operation by considering the energy absorption rate of the crystal, the population density in the ground state and the effective area ratio of the gain medium to the SA. Based on the simulation results, experiments have been carried out and it has been shown that the pulse timing jitter was reduced when a high spatial overlap coefficient was obtained between the pump mode and the laser mode in the gain medium. The experimental results agree with the simulations. Finally, a time jitter of 200 ns was achieved with a pulse repetition rate of 357 kHz under a CW LD pump power of 4.5 W. This work shows that 1.34 μm passively Q-switched laser can obtain high-repetition-rate stable pulse output while achieving small size, simple structure and low cost, which provides conditions for integration. It also provides a basis for realizing stable pulse output at higher repetition rates.

Funding information

This research was funded by Science and Technology Development Project of Jilin Province (grant numbers 20210201028GX, 20220508036RC).

CRediT authorship contribution statement

Yanxin Shen: Conceptualization, Methodology, Software, Investigation, Formal analysis, Writing – original draft. **Xihong Fu:** Data curation, Writing – original draft, Conceptualization, Funding acquisition, Resources, Supervision, Writing – review & editing. **Xinpeng Fu:** Visualization, Investigation, Funding acquisition. **Cong Yao:** Resources. **Wenyuan Li:** Software, Validation. **Jun Zhang:** Visualization, Writing – review & editing. **Yongqiang Ning:** Conceptualization, Funding acquisition, Resources, Supervision.

Declaration of Competing Interest

The authors declare that they have no known competing financial interests or personal relationships that could have appeared to influence the work reported in this paper.

Data availability

Data will be made available on request.

References

[1] Y.H. Zheng, Z.Q. Wu, M.R. Huo, H.J. Zhou, Generation of a continuous-wave squeezed vacuum state at 1.3 μm by employing a home-made all-solid-state laser as pump source, Chin. Phys. B. 22 (09) (2013) 431–434.
[2] W. Zhu, Q. Liu, Y. Wu, Aerosol absorption measurement at SWIR with water vapor interference using a differential photoacoustic spectrometer, Opt. Express. 23 (18) (2015) 23108–23116.
[3] Y.Y. Ma, J.X. Feng, Z.J. Wan, Y.H. Gao, K.S. Zhang, Continuous variable quantum entanglement at 1.34 μm, Acta Phys. Sin. 66 (24) (2017) 86–91.
[4] J. K. Thomas, W. A. Clarkson, R.K. Shori, 1.34 μm Nd:YVO_4 laser passively Q-switched by V:YAG and optimized for lidar. In *Solid State Lasers XXIX: Technology and Devices*, SPIE: San Francisco, CA,USA, 2020; Vol. 11259.
[5] J.L. Xu, H.T. Huang, J.L. He, J.F. Yang, B.T. Zhang, X.Q. Yang, F.Q. Liu, Dual-wavelength oscillation at 1064 and 1342 nm in a passively Q-switched Nd:YVO_4 laser with V^{3+}:YAG as saturable absorber, Appl. Phys. B. 103 (1) (2011) 75–82.
[6] S. Gao, Thermal effect and the passively Q-switching characteristics based on the composite YVO4/Nd:YVO_4 laser at 1342 nm, Mod. Phys. Lett. B 30 (7) (2016) 1650073.
[7] Y.X. Shen, X.P. Fu, C. Yao, W.Y. Li, Y.B. Wang, X.R. Zhao, X.H. Fu, Y.Q. Ning, Optical crystals for 1.3 μm all-solid-state passively Q-switched laser, Crystals 12 (8) (2022) 1060.
[8] H.C. Lai, A. Li, K.W. Su, M.L. Ku, Y.F. Chen, K.F. Huang, InAs/GaAs quantum-dot saturable absorbers for diode-pumped passively Q-switched Nd-doped 1.3-μm lasers, Opt. Lett. 30 (5) (2005) 480–482.
[9] H.Y. Lin, M.J. Zhao, H.J. Lin, Y.P. Wang, Graphene-oxide as saturable absorber for a 1342 nm Q-switched Nd:YVO_4 laser, Optik. 135 (2017) 129–133.
[10] S.P. Ng, D.Y. Tang, L.J. Qin, X.L. Meng, Z.J. Xiong, Period-doubling route to chaos in diode-pumped passively Q-Switched Nd : $GdVO_4$ and Nd : YVO_4 lasers, Int. J. Bifurcat. Chaos. 16 (9) (2006) 2689–2696.
[11] Y.-B. Wang, S. Wang, G.-Y. Feng, S.-H. Zhou, Laser diode-pumped low timing jitter saturable output coupler Q-switched microchip laser: simulations and experiments, Opt. Eng. 56 (08) (2017) 1.
[12] S. Wang, Y.B. Wang, G.Y. Feng, S.H. Zhou, A low timing jitter picosecond microchip laser pumped by pulsed LD, Opt. Commun. 371 (2016) 72–75.
[13] L.H. Zheng, A. Kausas, T. Taira, >MW peak power at 266 nm, low jitter kHz repetition rate from intense pumped microlaser, Opt. Express. 24 (25) (2016) 28748–28760.
[14] W.Y. Wang, M.L. Gong, X.Z. Liu, G.F. Jin, Stability of Passively Q-switched Solid-state Lasers and Pre-pumping Mechanism, Laser & Infrared. 02 (2000) 74–77.
[15] A.F. Shatalov, F.A. Shatalov, Reduction of the pulse repetition period jitter of a diode-pumped passively Q-switched solid-state laser, Radiophys Quantum El 52 (4) (2009) 305–310.
[16] S.-L. Huang, T.-Y. Tsui, C.-H. Wang, F.-J. Kao, Timing Jitter Reduction of a Passively Q-Switched Laser, Jpn. J. Appl. Phys. 38 (3A) (1999) L239.
[17] B. Cole, J. Lei, T. DiLazaro, B. Schilling, W. Trussell, L. Goldberg, In Reduction in timing jitter for a Cr:YAG Q-switched Nd:YAG laser, Proc.SPIE of Conference (2010).
[18] P.-L. Huang, C.-R. Weng, H.-Z. Cheng, S.-L. Huang, A Passively Q-Switched Laser Constructed by a Two-Mirror Reentrant Ring Cavity, Jpn. J. Appl. Phys. 40 (5B) (2001) L508.
[19] Y.F. Chen, P.Y. Chien, C.C. Lee, K.F. Huang, H.C. Liang, Timing jitter reduction of passively Q-switched solid-state lasers by coupling resonance between pumping and firing rates, Opt Lett. 45 (10) (2020) 2902–2905.
[20] Y. Lang, Y.Z. Chen, H.B. Zhang, J.G. Xin, W.Q. Ge, L.F. Liao, Z.W. Fan, Passively Q-switched laser based on Nd:YAG/YAG Polygonal Active Mirror with timing jitter improvement, Opt. Commun. 435 (2019) 81–87.
[21] X. Yan, Q. Liu, L. Huang, Y. Wang, X. Huang, D. Wang, M. Gong, A high efficient one-end-pumped TEM00laser with optimal pump mode, Laser Phys. Lett. 5 (3) (2008) 185–188.
[22] X. Wushouer, H.J. Yu, P. Yan, M.L. Gong, Investigation on mode matching including thermal effects in LD end-pumped passively mode-locked Nd/YVO4 laser, Chin. Opt. Lett. 8 (10) (2010) 1004–1007.
[23] Y.F. Chen, T.S. Liao, C.F. Kao, T.M. Huang, K.H. Lin, S.C. Wang, Optimization of fiber-coupled laser-diode end-pumped lasers: Influence of pump-beam quality, IEEE J. Quantum Electron. 32 (11) (1996) 2010–2016.
[24] J.J. Degnan, THEORY OF THE OPTIMALLY COUPLED Q-SWITCHED LASER, IEEE J. Quantum Electron. 25 (2) (1989) 214–220.
[25] Rüdiger Paschotta , Encyclopedia of Laser Physics and Technology.https://www.rp-photonics.com/doping_concentration.html (accessed 1 July 2006).
[26] J.A. Zheng, S.Z. Zhao, Q.P. Wang, Influence of thermal effect in gain-medium on optimum design od LD-End pumped solid state laser, Acta Photon. Sin. 30 (6) (2001).
[27] Q. Liu, X. Fu, M.L. Gong, L. Huang, Effects of the temperature dependence of absorption coefficients in edge-pumped Yb:YAG slab lasers, J. Opt. Soc. Am. B. 24 (9) (2007) 2081–2089.
[28] M. Lu, C.R. Chatwin, R.C.D. Young, P.M. Birch, Numerical simulation of a CW-pumped Cr:YAG passively Q-switched Yb:YAG pulsed laser, Opt. Lasers Eng. 47 (6) (2009) 617–621.
[29] X.Y. Zhang, S.Z. Zhao, Q.P. Wang, B. Ozygus, H. Weber, Modeling of passively Q-switched lasers, J. Opt. Soc. Am. B-Opt. Phys. 17 (7) (2000) 1166–1175.
[30] Y. F. Chen, M. X. Hsieh, Y. C. Tu, C. C. Lee, Y. T. Yu, C. H. Tsou, H. C. Liang, Pedagogically fast model to evaluate and optimize passively Q-switched Nd-doped solid-state lasers, Opt Lett. 46 (7)(2021), 1588-1591.